INVERSION OF SOIL STRUCTURE AND ANALYSIS OF THE SEISMIC WAVEFIELD FROM A VERTICAL ARRAY

F.J. Chávez-García[1] and D. Raptakis[2]

[1] *Professor, Dept. of Engineering Seismology, Institute of Engineering, Universidad Nacional Autónoma de México, Mexico*

[2] *Assist. Professor, Dept. of Civil Engineering, Aristotle University of Thessaloniki, Thessaloniki, Greece*
Email: paco@pumas.ii.unam.mx, raptakis@civil.auth.gr

ABSTRACT :

Currently, considerations of site effects in codes account for impedance contrast effects but do not consider the effects of laterally irregular structures. We need a better understanding of the relation between irregular subsoil structure, diffracted wavefield, and intensity measures. In this paper we analyze the wavefield that propagates in Euroseistest, a small basin in Northern Greece where a natural scale laboratory for seismology and earthquake engineering has been in operation for the last 15 years. The geometry and properties of the subsoil formations are well determined and a permanent accelerograph network, including a vertical array of six triaxial accelerometers is in operation. We present the preliminary results of the analysis of eight earthquakes recorded by this array using two approaches. We first use simulated annealing to minimize the difference between spectral ratios between neighbouring accelerometers and those computed using a 1D model. This allows us to improve previous determinations of seismic velocities and *Q* factors in the soil layers. The second approach is seismic interferometry. The analysis of traces deconvolved either with the surface or bottom records gives us further constraints on the subsoil structure and on the nature of the recorded waves. Our results are useful to improve the soil profile. The analysis of the records shows that local structure conditions the recorded wavefield independently of the source location. Thus, the consideration of the lateral heterogeneity is essential to predict ground motion at this site.

KEYWORDS: site effects, alluvial basins, spectral ratios, inversion, interferometry

1. INTRODUCTION

Site effects frequently condition damage distribution during large earthquakes. In closed basins, it is not only the vertical heterogeneity that contributes to ground motion amplification. Lateral irregularities add to the complexity of the recorded wavefield through the generation of surface waves. Up to now, it is not possible to predict in detail ground motion for future events because it is not simple to predict the interactions between the incident waves and a complex geometry (e.g., Chávez-García, 2007). Computation of those interactions require not only a detailed knowledge of the incident waves but also a detailed knowledge of the subsoil structure, both geometry and mechanical properties, of the media through which those waves propagate. For this reason, test sites have been developed, where thorough subsoil investigations may be related to the effects of lateral heterogeneity on ground motion. Later, the understanding gained can be used in other, less knows sites.

Euroseistest is a very long running experimental site for the study of site effects. It is a small valley located in northern Greece (Figure 1). Since the early 1990's, this site was selected for a series of EU funded research projects. Comprehensive geophysical exploration campaigns, as well as seismic instrumentation using temporary and permanent networks, have provided large quantities of useful information concerning its structure and soil response. The results have appeared in many publications (e.g., Raptakis et al., 1998, 2000; Jongmans et al., 1998; Riepl et al. 1998; Pitilakis et al., 1999; Chávez-García et al., 2000). These publications have presented the structure of the valley and confronted its observed seismic response with 1D and 2D modelling results. They have shown that the response of Euroseistest valley cannot be understood using the 1D paradigm and need to be analysed using, at least, 2D models.

Seismic instrumentation at Euroseistest has varied along its history. However, a permanent accelerograph array has been in operation for several years now. One component is a vertical array at the centre of the valley which consists of six 3-axial accelerographs. In this paper we use data recorded by this array to make a preliminary exploration of the structure at the centre of the valley, and the nature of the wavefield that has been recorded there. With this aim, we present, first, an inversion of spectral ratios between neighbouring stations of the vertical array. This allows us to find the 1D structure at the centre of the valley that best explains the observations. Second, we use seismic interferometry (Snieder and Safak, 2006) to investigate the the recorded wavefield. Our results are useful to improve the soil profile, which will be used later in simulations of the seismic response of the valley in 2D and 3D models. In addition, the analysis of the records shows that local structure conditions the recorded wavefield independently of the source location. Thus, consideration of the lateral heterogeneity of the valley is essential to predict ground motion at this site.

2. DATA

We use data recorded by the vertical array at the centre of Euroseistest. As part of its permanent instrumentation, a surface array of accelerographs operates at the 2D cross-section that was chosen in the first stage of the Euroseistest projects (Figure 2). (An additional line of surface instruments has been installed along the main valley axis, perpendicularly to Figure 2, see Raptakis et al., 2005.) In addition to those instruments, a vertical accelerograph array operates at its centre, under station TST (Figure 2). Five borehole accelerographs record ground motion at the depths of 21, 40, 72, 136, and 196 m. The geometry, mechanical properties, and seismic response of the different sedimentary layers have been investigated in detail. Figure 3 shows the stratigraphy at TST. The properties of the layers are given in Table 2.1.

We have used data from eight small events ($3.1 \leq M_L \leq 4.3$). All of them were well recorded by the 6 stations of the vertical array. A 20-sec time window was extracted, centred on the S-wave package. Fourier amplitude spectra were computed after applying a baseline correction and a 10% taper to the extracted window. The amplitude spectra were smoothed using a Hanning window. Spectral ratios were calculated between neighbouring stations, for each component: vertical and radial and transverse relative to the main axis of the valley. Finally, the average spectral ratio for each component was computed as the average for all events.

Table 2.1 Initial properties of the 1D profile at TST

Layer	H [m]	V_S [m/s]	V_P [m/s]	ρ [gr/cm3]
A	3.0	130.0	410.9	2.05
B	16.0	200.0	1162.1	2.15
C	30.0	300.0	1365.0	2.08
D	31.0	450.0	1441.4	2.10
E	50.0	650.0	1915.0	2.16
F	54.0	800.0	2243.9	2.20
G*	10.0	1250.0	2563.0	2.50
G	-	2600.0	3992.4	2.60

3. INVERSION OF SPECTRAL RATIOS

3.1. Adaptive Simulated Annealing (ASA) Algorithm

Algorithms based on simulated annealing (SA) are general Monte Carlo approximation methods that allow optimizing problems when a desired global minimum is hidden among many local minima. This is especially useful when the relation between the parameters and the objective function is highly non-linear. SA is a search algorithm where the size of the parameter space that is sampled is reduced progressively. The amount of possible change in the parameters is controlled using an analogy with the annealing process in metallurgy;

higher temperatures allow larger changes. As the metal cools down, the possible changes to its crystalline structure are smaller. In the SA algorithm, as the search for the minimum narrows to a small range of the parameters, the possible changes to them are smaller. Adaptive simulated annealing (ASA) is an extension of SA which explores the parameter space in a more efficient way, decreasing significantly the computational effort (e.g., Ingber, 1989; Ingber and Rosen, 1992). The ASA algorithm used in this study is that of Ingber (1989) and our study follows closely that of Satoh (2006), where the details of the method are described.

3.2. Objective Function

The objective function is the function to be minimized through the ASA algorithm. This function quantifies the difference between observed and computed spectral ratios as a function of a parameter vector $\bar{x}$. In terms of their depths, we compute spectral ratios for station pairs 0-21, 21-40, 40-72, 72-136, and 136-196. Let O_{jk} be the observed average spectral ratio for S-wave amplitude spectra of component j between the two stations forming the k^{th} station pair. We minimize its difference with the equivalent computed spectral ratio, M_{jk}. Synthetic spectral ratios are computed using the Thomson-Haskell matrix method (Aki and Richards, 1980), which allows including all upgoing and downgoing waves, as is the case for the observed ratios. Haskell's method allows to compute that ratio given an incident wave (P or S) with a given incident angle at the base of the stratigraphy. Our objective function is given by

$$E(\bar{x}) = \frac{1}{5}\left\{\sum_{k=1}^{5}\left[\sum_{j=1}^{3}\left(\frac{\sum_{i=imin}^{imax}\left|\frac{M_{jk}(f_i)-O_{jk}(f_i)}{w(f_i)}\right|}{\sqrt{\sum_{i=imin}^{imax}\frac{M_{jk}(f_i)}{w(f_i)}\sum_{i=imin}^{imax}\frac{O_{jk}}{w(f_i)}}}+\frac{\sum_{i=imin}^{imax}\left|\frac{\log_{10}M_{jk}(f_i)-\log_{10}O_{jk}(f_i)}{w(f_i)}\right|}{\sqrt{\sum_{i=imin}^{imax}\frac{\log_{10}M_{jk}(f_i)}{w(f_i)}\sum_{i=imin}^{imax}\frac{\log_{10}O_{jk}(f_i)}{w(f_i)}}}\right)\right]\right\} \quad (3.1)$$

where i is the index for frequencies, j is the index for components, k is the index for station pairs, and $w(f_i)$ is a weight function given by (Satoh, 2006)

$$w(f_i) = \frac{1}{\log_{10} f_i - \log_{10} f_{i-1}} \quad (3.2)$$

The initial model is given in Table 2.1. In order to reduce the number of parameters, the thickness (H) and density (ρ) of each layer was considered fixed, and Q_S is modelled as a function of frequency, f, and V_S, shear wave velocity, using

$$Q_S = \frac{V_S}{b} f^a \quad (3.3)$$

where f is in Hz and V_S in m/s. a and b are constants to be inverted. Q_P was taken as twice Q_S. The number of parameters to be inverted is 19: eight values for V_S, eight values for V_P, the incidence angle and the two attenuation parameters, a and b. ASA inversion requires the specification of a finite range of variation for each parameter. Velocities, V_S and V_P, were allowed to vary within 70 to 130% of the initial value. The incidence angle was allowed to take any value between 0 and 40 while the attenuation parameters had a range of 0 to 2 for a and 0 to 4 for b. Within those ranges, ASA generates many possible parameter vectors using a random number generator. We made the inversions using five different seeds for each case.

3.3. Results

An example of the results is shown in Figure 4. We assumed incidence of S-waves and, therefore, simulated vertical motion results only from the oblique incidence of S-waves. The solid line shows the observed spectral ratios between station pairs. The dashed line shows the corresponding computed spectral ratios using the stratigraphy obtained from one of the ASA inversions. We observe a good agreement between observed and computed spectral ratios for the radial and transverse components, especially for the topmost layers and for frequencies smaller than 5 Hz (this is due to our weight scheme). The results in the third column show

clearly that the spectral ratios for the S-wave window of the vertical component cannot be explained using S-wave incidence. Contrary to Satoh (2006), our results suggest that vertical components consist mostly of P waves; either P waves still dominate in the vertical component S-wave window or they are converted from S at a deep interface. For this reason, we inverted independently the spectral ratios for the vertical component, assuming incidence of P waves. The results are shown in Figure 5. The thick line shows the observed spectral ratios, while the different thin lines show the synthetic ratios computed using the 1D profiles that result from the ASA inversions. Each line corresponds to a different seed for the random number generator. We observe a very good agreement between observations and synthetics. The incidence angle obtained from the inversions was larger than 30°, suggesting that the vertical component of the S-wave window consists mainly of P-waves converted from S at an interface deeper than our deepest accelerometer. These P-waves are later propagated without significant wave conversions. We fixed the V_P and Q_P values obtained from the inversion of the vertical component spectral ratios, and used them in the inversions of the radial and transverse component spectral ratios. The final results are given in Table 3.1. The Q factors of the deeper layers are not well constrained because of the short (in terms of wavelength) path between stations. However, the other values are well constrained. The resulting 1D profile will be used later to assign properties to the different layers and compute the response for 2D and 3D models of the whole valley. This work is under way.

Table 3.1. Final properties of the 1D profile at TST

Layer	H [m]	V_S [m/s]	V_P [m/s]	Q_S	Q_P
A	3.0	104.0	296.0	112	106
B	16.0	166.0	1160.2	4	196
C	30.0	227.0	1322.9	5	238
D	31.0	315.0	1458.3	138	304
E	50.0	455.0	1764.2	233	414
F	54.0	560.0	2160.1	545	46
G*	10.0	875.0	2481.9	470	5
G	-	2868.0	3920.6	827	10

4. SEISMIC INTERFEROMETRY

A different way to analyse the data of the vertical accelerograph array at Volvi is the use of seismic interferometry. This technique is based on the correlation of waves recorded at different receivers. This approach is valuable because it enables the study of the waves that propagate between receivers without needing a source at one of the receiver locations. It does not matter whether the waves recorded at the receivers are excited by coherent or incoherent sources.

We follow the procedure described in detail in Snieder and Safak (2006). We analyse our data in time domain by deconvolving the waves recorded at all stations by the signal recorded at the surface. The deconvolution of signal $u_1(\omega)$ by the signal $u_2(\omega)$ is given by

$$D(\omega) = \frac{u_1(\omega)u_2^*(\omega)}{|u_2(\omega)|^2+\varepsilon} \tag{4.1}$$

where the asterisk denotes complex conjugate. ε is a small constant, added to the denominator, to avoid the instabilities introduced by the notches in the spectrum of u_2. Following Snieder and Safak (2006), we set ε to be 10% of the average spectral power of u_2.

An example of the results is given in Figure 6, for the transverse component and one of the eight events we analysed. The traces at all depths were deconvolved against the trace at the surface. The deconvolved trace at the surface is a single spike because a signal deconvolved with itself is a delta function. The traces at the other depths show clearly the incident S pulse travelling upwards as well as that one reflected at the free

surface propagating downwards. The amplitude relation between each pulse is a function of the amplification along the profile, due to the S-wave velocity decreasing towards the surface, and the attenuation due to anelasticity. The rapid disappearance of the downward pulse indicates the large effect of amplification present in the profile. Contrary to Snieder and Safak (2006), we do not observe common wavetrains in the deconvolved traces. The reason is that those authors analysed seismic motion recorded at different levels of a building. Millikan library, studied by Snieder and Safak (2006) is mostly homogeneous all along its height. In contrast, our soil profile is highly heterogeneous vertically and the surface wave modes (akin to fundamental mode resonances of the building) have a more complicated structure.

We analysed the deconvolved waveforms obtained using anyone of our traces as master. The results allowed us to constrain the shear-wave velocities between stations. They also provided additional constraints on the attenuation factors for the layers of the profile. These results were not significantly different from the values reported in Table 3.1 obtained from ASA inversions.

5. CONCLUSIONS

We have presented the preliminary results of the analysis of earthquake data recorded at the vertical array in Euroseistest. Eight events that were well recorded by the six 3-axial accelerographs that form that array were analysed using two different approaches. The first one was the inversion of a 1D stratigraphic profile that best explained the spectral ratios observed between neighbouring stations. It was not possible to invert simultaneously horizontal and vertical component spectral ratios. That is, vertical component spectral ratios could not be explained assuming S-wave incidence at the base of the profile. The independent inversion of the vertical components allowed to obtain reliable V_P and Q_P values for the profile, and also suggested that vertical components for the S-wave window consist of P-waves converted from S at an interface deeper than our deepest accelerograph. The final results explained well all our data, in terms of spectral ratios. The final profile will be used in 2D and 3D simulations of ground motion for the whole valley.

The second approach used was seismic interferometry. The analysis of traces deconvolved either with the surface or bottom records gives us further constraints on the subsoil structure and on the nature of the recorded waves. Our results are useful to confirm the soil profile properties derived from the ASA inversions, which will be used later in simulations of the seismic response of the valley in 2D and 3D models. In addition, the analysis of the records shows that local structure conditions the recorded wavefield independently of the source location. This indicates that the consideration of the lateral heterogeneity of the valley is essential to predict ground motion at this site

ACKNOWLEDGEMENTS

We thank K. Pitilakis for his continuing role as coordinator of Euroseistest, overseeing the projects that have contributed useful data and results. The installation and maintenance of the network have benefited from the dedication of A. Marino and N. Adam from ITSAK. Signal processing benefited from SAC (Goldstein et al., 2003). This research was supported by Conacyt, Mexico, through contract SEP-2003-C02-43880/A.

REFERENCES

Aki, K. and Richards, P.G. (1980). Quantitative seismology. Theory and methods, Freeman and Co., San Francisco.
Chávez-García, F.J. (2007). Site effects: from observation and modelling to accounting for them in building codes, en K.D. Pitilakis (ed.) Earthquake Geotechnical Engineering, 4th International Conference of Earthquake Geotechnical Engineering - Invited lectures, vol. 6 de la serie Geotechnical, Geological and Earthquake Engineering, ISBN: 978-1-4020-5 892-9, ISSN 1573-6059, DOI 10.1007/978-1-4020-5893-6,

Springer, 53-72.
Chávez-García, F.J., Raptakis, D., Makra, K., and Pitilakis, K. (2000). Site effect at Euroseistest-II. Results from 2D numerical modeling and comparison with observations. Soil Dyn. Earthq. Engrg. 19:1, 23–39.
Goldstein, P., Dodge, D., Firpo, M., and Minner, L. (2003). SAC2000: Signal processing and analysis tools for seismologists and engineers, Invited contribution to The IASPEI International Handbook of Earthquake and Engineering Seismology, Edited by WHK Lee, H. Kanamori, P.C. Jennings, and C. Kisslinger, Academic Press, London.
Ingber, L. (1989). Very fast simulated reannealing. Math. Comp. Modeling 2, 967–973.
Ingber, L., and Rosen, B.E. (1992). Genetic algorithms and very fast simulated reannealing: a comparison. Math. Comp. Modeling 16, 87–100.
Jongmans, D., Pitilakis, K., Demanet, D., Raptakis, D., Riepl, J., Horrent, C., Tsokas, G., Lontzetidis, K., and Bard, P.-Y. (1998). EURO-SEISTEST: determination of the geological structure of the Volvi graben and validation of the basin response. Bull. Seism. Soc. Am. 88, 473–87.
Pitilakis, K., Raptakis, D., Lontzetidis, K., Tika-Vassilikou, T., and Jongmans, D. (1999). Geotechnical and geophysical description of EURO-SEISTEST, using field, laboratory tests and moderate strong motion recordings. J. Earthq. Engrg. 3:3, 381–409.
Raptakis, D., Theodulidis, N., Pitilakis, K. (1998). Data analysis of the EUROSEISTEST strong motion array in Volvi (Greece): standard and horizontal to vertical spectral ratio techniques. Earthq. Spectra 14:1, 203–24.
Raptakis, D., Chávez-García, F.J., Makra, K., and Pitilakis, K. (2000). Site effect at Euroseistest-I. Determination of the valley structure and confrontation of observations with 1D analysis. Soil Dyn. Earthq. Engrg. 19:1, 1–22.
Raptakis, D.G., Manakou, M.V., Chávez-García, F.J., Makra, K.A., and Pitilakis, K.D. (2005). 3D configuration of Mygdonian basin and preliminary estimate of its seismic response. Soil Dyn. Earthq. Engrg. 25, 871-887.
Riepl, J., Bard, P.-Y., Papaioannou C., and Nechtschein, S. (1998). Detailed evaluation of site response estimation methods across and along the sedimentary valley of Volvi (EURO-SEISTEST). Bull. Seism. Soc. Am. 88, 488–502.
Satoh, T. (2006). Inversion of Qs of deep sediments from surface-to-borehole spectral ratios considering obliquely incident SH and SV waves. Bull. Seism. Soc. Am. 96, 943-956.
Snieder, R. and Safak, E. (2006). Extracting the building response using seismic interferometry: theory and application to the Millikan library in Pasadena, California. Bull. Seism. Soc. Am. 96, 586-598.

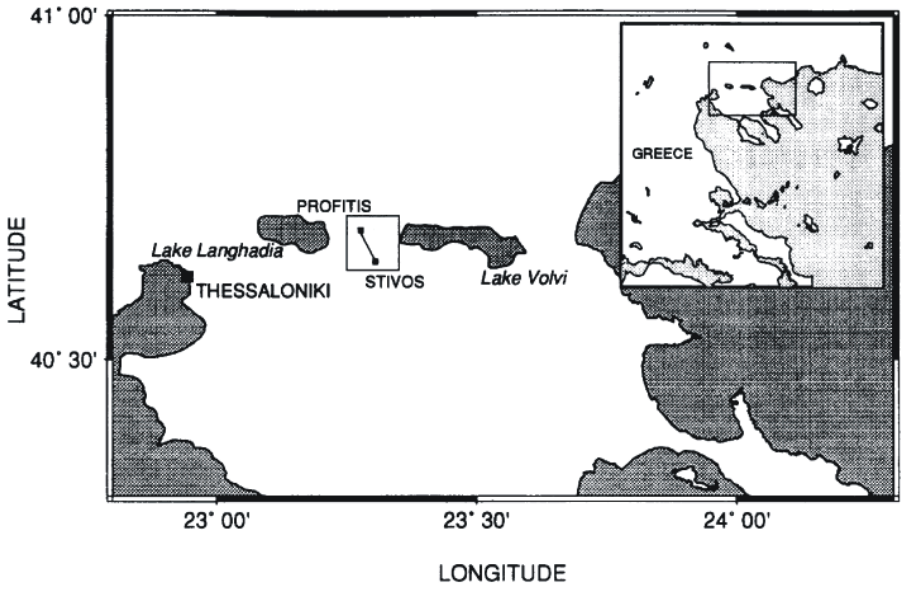

Figure 1 Location of the profile Profitis-Stivos in northern Greece. This profile cuts the Volvi valley, between lakes Langhadia and Volvi ans was chosen as the 2D section to investigate site effects in a laterally heterogeneous structure. [After Chávez-García et al., 2000.]

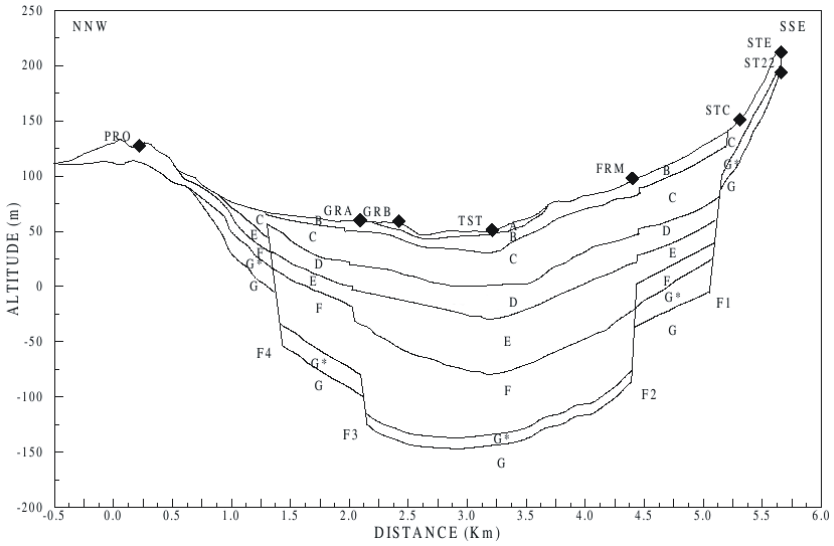

Figure 2 Geological profile along the section Profitis-Stivos indicated in the previous figure. The properties of the different layers (A to G) are given in Table 1. The solid diamonds indicate the location of the surface accelerometers of the permanent array. [After Chávez-García et al., 2000.]

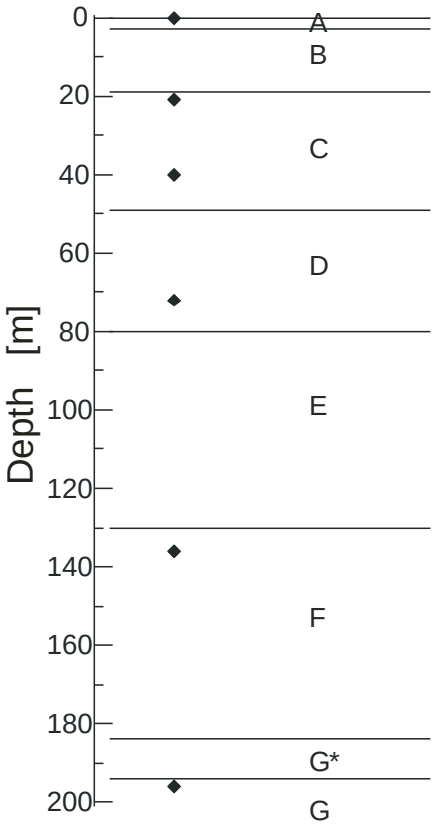

Figure 3 1D structure at the center of the Euroseistest valley, at the location of TST in the previous figure. The properties of the different layers (A to G) are given in Table 1. The solid diamonds indicate the location of the stations that form the vertical array.

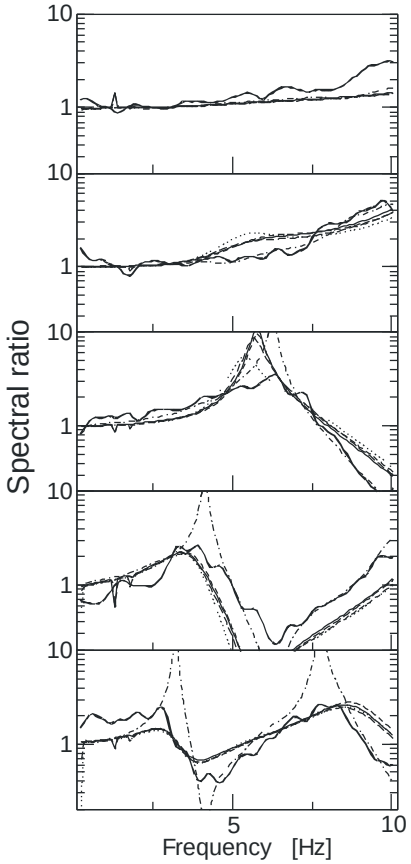

Figure 5 Example of the comparison between observed spectral ratios (thick lines) and those computed using the 1D profile derived from an ASA run (thin lines). Only the vertical component ratios were inverted using incidence of P waves.

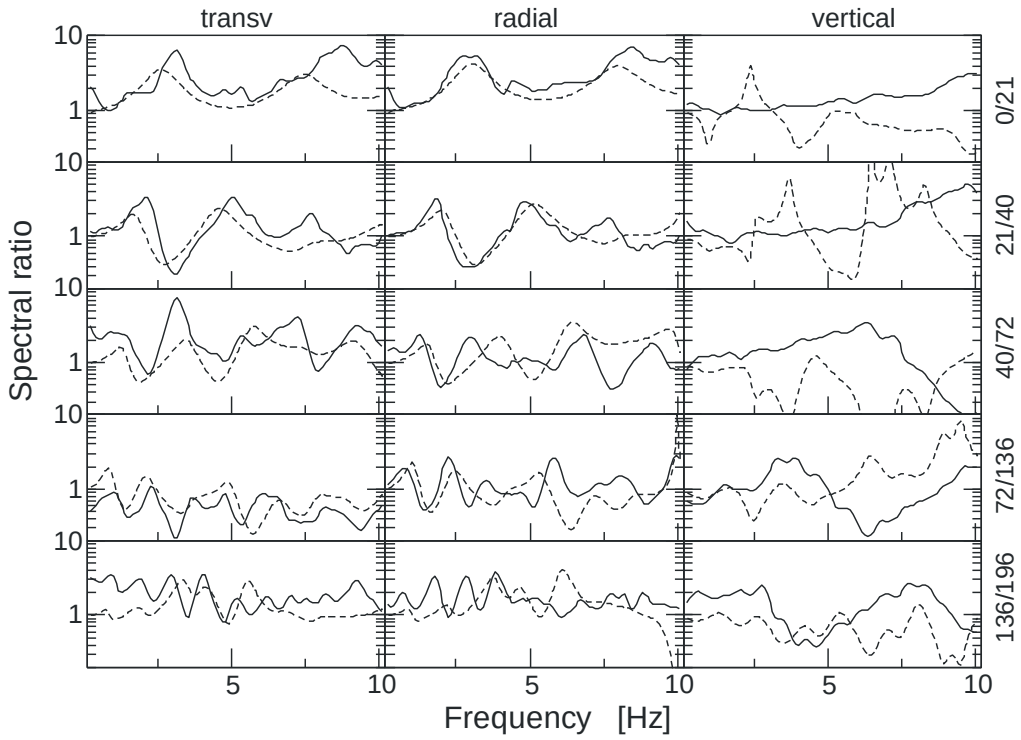

Figure 4 Example of the comparison between observed spectral ratios (solid lines) and those computed using the 1D profile derived from an ASA run (dashed lines).Each column corresponds to a component of ground motion, while the lines correspond to different station pairs (indicated to the right).

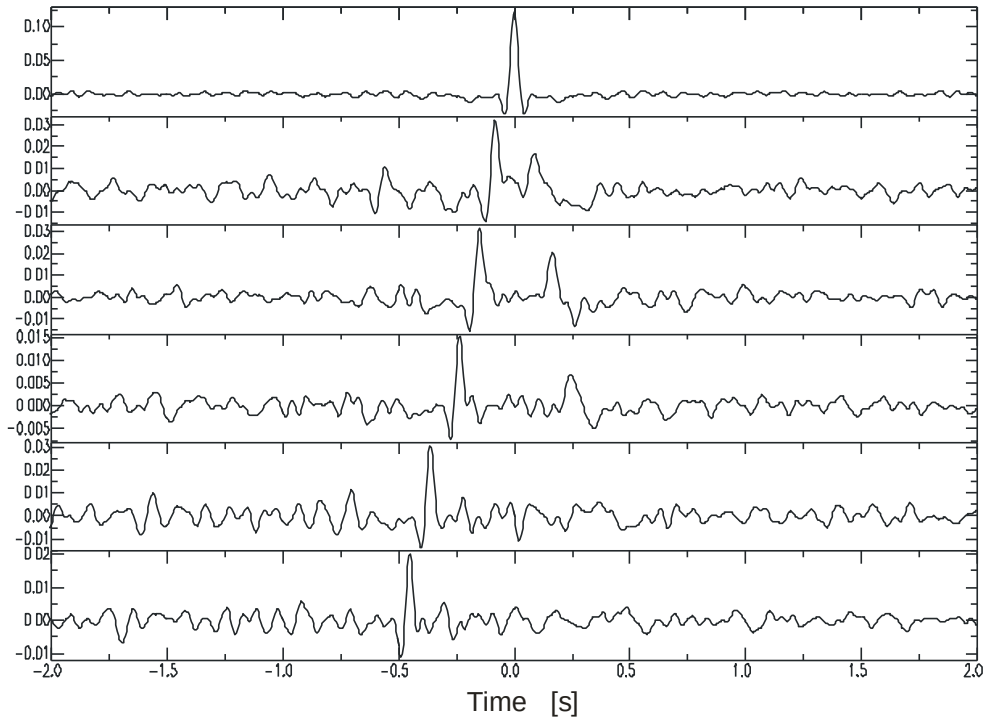

Figure 6 Traces recorded by the vertical array deconvolved by the record obtained at the free surface. These results correspond to transversal components recorded for a small event that occurred on 15/07/04, 11 km to the South of TST. The main features are the upgoing S pulse and its downgoing reflection at the free surface.